

## Article

# Multi-Omics Analyses to Identify FCGBP as a Potential Predictor in Head and Neck Squamous Cell Carcinoma

Yu-Hsuan Lin <sup>1,2,3,4</sup> , Yi-Fang Yang <sup>5</sup>  and Yow-Ling Shiue <sup>1,6,\*</sup> 

<sup>1</sup> Institute of Biomedical Sciences, National Sun Yat-sen University, Kaohsiung 804, Taiwan; lucaslinyin@gmail.com

<sup>2</sup> Department of Otolaryngology, Head and Neck Surgery, Kaohsiung Veterans General Hospital, Kaohsiung 813, Taiwan

<sup>3</sup> School of Medicine, National Yang Ming Chiao Tung University, Taipei 112, Taiwan

<sup>4</sup> School of Medicine, Chung Shan Medical University, Taichung 402, Taiwan

<sup>5</sup> Department of Medical Education and Research, Kaohsiung Veterans General Hospital, Kaohsiung 813, Taiwan; yvonne845040@gmail.com

<sup>6</sup> Institute of Precision Medicine, National Sun Yat-sen University, Kaohsiung 804, Taiwan

\* Correspondence: shirley@imst.nsysu.edu.tw; Tel.: +886-7-525-2000; Fax: +886-7-525-0197

**Abstract: (Purpose)** Previous studies have pointed out the significance of IgG Fc binding protein (FCGBP) in carcinogenesis, cancer progression, and tumor immunity in certain malignancies. However, its prognostic values, molecular interaction, and immune characteristics in the head and neck squamous cell carcinoma (HNSC) remained unclear. **(Methods)** To evaluate the potential role of the *FCGBP* gene, we used GEPIA2 and UALCAN platforms to explore the differential levels, survivals, and genetic alteration through cBioPortal (based on The Cancer Genome Atlas dataset). STRING, GeneMania, and TIMER2.0 identified the interacting networks. LinkedOmics performed Gene enrichment analysis, and TISIDB and TIMER2.0 evaluated the role of *FCGBP* in the tumor microenvironment. **(Results)** The expression level of *FCGBP* is lower in cancer tissues. A high *FCGBP* level is significantly associated with better overall- and disease-specific-survivals, regardless of human papillomavirus infection. Low *FCGBP* levels correlated to a higher tumor protein *p53* (*TP53*) mutation rate ( $p = 0.018$ ). *FCGBP* alteration significantly co-occurred with that of *TP53* ( $q = 0.037$ ). Interacting networks revealed a significant association between FGF13 and trefoil factor 3 (TFF3), a novel prognostic marker in various cancers, at transcriptional and translational levels. Enrichment analyses identified that the top gene sets predominantly related to immune and inflammatory responses. Further investigation found that the *FCGBP* mRNA level positively correlated to the infiltration rates of B cells, Th17/CD8+ T lymphocytes, T helper follicular cells, mast cells, and expression levels of various immune molecules and immune checkpoints in HNSC. **(Conclusions)** We found that the *FCGBP* mRNA level negatively correlated to *TP53* mutation status while positively correlated to the *TFF3* level. Additionally, FCGBP may regulate the tumor microenvironment. These findings support the *FCGBP* as a potential biomarker to estimate HNSC prognoses.

**Keywords:** head neck squamous cell carcinoma; IgG Fc binding protein; FCGBP; prognosis; tumor microenvironment; immune



**Citation:** Lin, Y.-H.; Yang, Y.-F.; Shiue, Y.-L. Multi-Omics Analyses to Identify FCGBP as a Potential Predictor in Head and Neck Squamous Cell Carcinoma. *Diagnostics* **2022**, *12*, 1178. <https://doi.org/10.3390/diagnostics12051178>

Academic Editors: Maciej Misiolok and Joanna Katarzyna Strzelczyk

Received: 23 March 2022

Accepted: 5 May 2022

Published: 9 May 2022

**Publisher's Note:** MDPI stays neutral with regard to jurisdictional claims in published maps and institutional affiliations.



**Copyright:** © 2022 by the authors. Licensee MDPI, Basel, Switzerland. This article is an open access article distributed under the terms and conditions of the Creative Commons Attribution (CC BY) license (<https://creativecommons.org/licenses/by/4.0/>).

## 1. Introduction

Head and neck squamous cell carcinoma (HNSC) ranks the 7th among cancer-related deaths, with over 890,000 new cases annually worldwide and mortality of approximately 50% [1]. Leading causes of HNSC include alcohol consumption, smoking, and high-risk human papillomavirus (HPV) infection [2]. Although the growing trend in HNSC may vary with ethnicities, the annual incidence of HPV-related HNSC is consistently increasing [2,3]. Cancer behaviors are distinct between HPV-related and HPV-unrelated HNSCs. Overexpression of cyclin-dependent kinase inhibitor 2A (CDKN2A/p16), downregulation

of tumor protein p53 (TP53), and inactivation of RB transcription corepressor 1 (RB1), have been characterized in HPV-related HNSC [4]. The underlying molecular mechanisms were identified as HPV oncoprotein E6 ubiquitinate TP53, another oncoprotein E7 eliminated RB1 through proteasomal degradation of RB1 to facilitate cell cycle progression, thereby transactivation of the *CDKN2A* via E2F proteins releasing from RB1/E2F family transcription factors [4]. In terms of clinical manifestations, HPV-related HNSC significantly correlated with favorable treatment responses after radiotherapy and chemotherapy, leading to a better prognosis [5]. Nevertheless, the overall survival (OS) of HNSC did not improve considerably despite multidisciplinary advances [5]. Consequently, it is essential to explore novel biomarkers for effective therapeutic strategies.

The *FCGBP* gene encoded a cysteine-rich glycoprotein comprising approximately 5400 amino acid residues, which may bind the Fc portion of the IgG molecule [6]. The mucous epithelia of various organs, including the intestine and colon, gallbladder, salivary gland(s), and cervix uterus, may synthesize FCGBP, thus becoming a constituent of many body fluids [6,7]. Physiologically, FCGBP protects the cells against infections from microorganisms [8]. One speculated mechanism is that FCGBP modulates the innate mucosal immunity to defense by binding the trefoil factor 3 (TFF3) [9]. The pathogenic roles of FCGBP in malignancy were firstly reported for its implication in ulcerative colitis [10], a condition that predisposes to colorectal cancer development [11]. Subsequent investigations have demonstrated the potential importance of *FCGBP* in several cancers [11–17]. *FCGBP* alternative splicing and *FCGBP* mutations may implicate the pathogenesis of lung cancer [12] and hepato-cholangiocarcinoma [13], respectively. Its protein is abnormally expressed in many malignancies, suggesting the potential role in tumorigenesis. In tissues from prostate adenocarcinoma in human and transgenic mice, FCGBP levels were significantly downregulated [14]. The *FCGBP* mRNA levels were significantly and differentially expressed in normal thyroid tissues, follicular- and papillary-thyroid carcinomas, with expression levels higher in adenoma and lower in carcinoma compared to that in normal tissues [15]. Moreover, the FCGBP protein served as an independent prognostic factor in gallbladder adenocarcinoma [16] and metastatic colorectal cancer [17]. The *FCGBP* level was one of the top differentially expressed transcripts between chemosensitive and chemoresistant tissues [18]. Accordingly, advanced ovarian serous adenocarcinomas applied *FCGBP* mRNA levels to predict therapy responses [18].

In HNSC-derived cell lines, *FCGBP* levels increased by overexpressing E6 and decreased after treatment with transforming growth factor-beta (TGF $\beta$ ) [19]. Similar to the conditions of the gallbladder- [16] and colorectal- [17] cancers, *FCGBP* may participate in regulating HNSC metastasis through epithelial-mesenchymal transition (EMT) [19]. Despite these findings, whether the *FCGBP* level affects immune infiltration or contributes to survival in HNSCs remains unclear. Exploring the roles of FCGBP is critical due to the tumor microenvironments' impact on carcinogenesis and tumor progression [20]. Another concern is that immunotherapy survival advantages in an HNSC subset may be attributable to factors including immune cells, immune mediators, and related pathways [21]. Consequently, we aimed to investigate the *FCGBP* genetic characterizations on the prognostic significance, the rationale of the impacts of molecular-molecular interaction, and immune features on clinical outcomes of HNSC through bioinformatics analysis.

## 2. Materials and Methods

### 2.1. Expression Feature Analysis

We explored the mRNA levels of *FCGBP* between cancerous and noncancerous tissues using the GEPIA2 platform [22] and evaluated the effects of *TP53* mutation and HPV infection statuses on differential *FCGBP* levels by TIMER2.0 [23] and UALCAN [24]. The correlations between diverse clinical factors and *FCGBP* levels on The Cancer Genome Atlas (TCGA) dataset were calculated by IBM SPSS Statistics for Windows, version 21 (IBM, Armonk, NY, USA). The abbreviations of different cancer types were based on TCGA Study Abbreviations (TCGA Study Abbreviations | NCI Genomic Data Commons

(<https://gdc.cancer.gov/>, accessed on 22 March 2022). The mass spectrometry proteomic profiles generated by the Clinical Proteomic Tumor Analysis Consortium (CPTAC) were the source for protein expression analyses [25]. UALCAN database examined the correlations between the FCGBP protein level and various clinical factors. Gene/transcript expression levels are presented as  $\log_2$  [transcripts per million (TPM)] or  $\log_2$  (TPM + 1) in GEPIA2;  $\log_2$  RNA-Seq by Expectation-Maximization (RSEM) in TIMER2.0. A  $p < 0.05$  is considered as statically significant.

### 2.2. Survival Prognosis Analysis

The prognosis analysis of the FCGBP level was conducted in GEPIA2 to generate the survival map and Kaplan-Meier curve for the overall- and disease-specific survival related to the FCGBP level from the TCGA dataset. The expression level in the top 50% (median) was considered the high-FCGBP group. To further test whether the prognostic significance of the FCGBP level was independent of other variables of HNSC, we performed univariate and multivariate Cox regressions analyses. The log-rank test compared the survival rates, with the significance threshold set at  $p < 0.05$ . Moreover, TIMER 2.0 generated the survival plots stratified by HPV infection.

### 2.3. Gene Alteration Analysis

We used the cBioPortal platform [26] to probe the association between different types of mutations and the FCGBP mRNA levels. After identifying the most frequently altered genes with FCGBP alteration, we estimated the genetic co-occurrence of these core genes with FCGBP alterations. Next, we verified the associations of the FCGBP level with the core genes using the “Gene\_Corr module” of TIMER2.0. After submission, the correlation curve(s) was generated automatically.

### 2.4. Molecular Interaction Analysis

We used the STRING database [27] to explore the protein-protein interaction of the FCGBP. We identified significant proteins by intersecting with the FCGBP associated co-expressed genes and then tested their correlation at the mRNA level. GeneMania [28] further validated the association between FCGBP and significant proteins. GeneMania provided information for the co-expression, co-localization, gene functions, and related pathways of appealing genes in addition to the gene-gene interaction.

### 2.5. Gene Set Enrichment Analysis

We used the LinkedOmics database [29] to download the mRNA dataset of HNSC patients and obtained a total of 517 cases containing whole FCGBP level and clinical features. After identifying 20,163 genes from 520 microarrays, a heat map presented the top 50 positively correlated transcripts to the FCGBP level. The co-expressed genes associated with the FCGBP level were selected for enrichment analysis to reflect the roles of FCGBP. We included a post-processing step targeting Gene Ontology (GO) to identify the most representative significant gene sets for visualization through redundancy reduction and affinity propagation cover. A  $p < 0.05$  determined significantly enriched terms. Gene Set Enrichment Analysis (GSEA) also highlighted the Kyoto Encyclopedia of Genes and Genomes (KEGG) pathways through analyzing a minimum number of genes (size) of 3 and a simulation of 500 within the HNSC dataset.

### 2.6. Immune Infiltration

First, we analyzed the associations of the FCGBP level with the immunomodulatory transcripts in TISIDB [30], and identified the immune cells with significant infiltrate estimation values correlated to the FCGBP level. The identified immune cells were next validated in TIMER2.0 using the ‘Immune\_Gene module’. We selected the immune cells that correlated significantly in the same directions using different algorithms, including TIMER, EPIC, QUANTISEQ, XCELL, MCP-COUNTER, CIBERSORT, and CIBERSORT-ABS. The

associations of respective markers of the significant tumor-infiltrating immune cells with the *FCGBP* level were further explored using the TIMER2.0 correlation module. Finally, we verified the correlations of the *FCGBP* level and immune-related molecules and immune checkpoints by the TISIDB database and TIMER2.0, respectively. The Spearman correlation test analyzed the associations, and a *p*-value less than 0.05 indicates statistical significance.

### 3. Results

#### 3.1. Downregulation of the *FCGBP* Level in Head and Neck Squamous Cell Carcinoma

To investigate the potential roles of the *FCGBP* gene in HNSC, we utilized TCGA dataset in GEPIA2, UALCAN, and TIMER2.0 to evaluate the *FCGBP* mRNA levels in tumoral and normal tissues. The *FCGBP* mRNA level from tumors was significantly lower than normal tissues (Figure 1A). However, we did not find a significant difference between HPV-related tumors ( $n = 41$ ) and normal tissues ( $n = 44$ ) and the *FCGBP* mRNA level ( $p = 5.2 \times 10^{-1}$ , Figure 1B). Table 1 demonstrates the correlations between the *FCGBP* level and critical clinical factors. By using the median value of *FCGBP* mRNA level to divide 442 HNSC patients into high- ( $n = 209$ ) and low- ( $n = 233$ ) *FCGBP* groups, we found a significant decrease in *FCGBP* level from American Joint Committee on Cancer (AJCC) T1/T2 to T3/T4 ( $p < 1 \times 10^{-3}$ ) and from stage I to stage IV ( $p = 1.5 \times 10^{-2}$ ) in patients with HNSC. Notably, we found a significant difference in *FCGBP* level between *TP53* mutation ( $n = 331$ ) and wild type ( $n = 168$ ). Furthermore, the Wilcoxon rank-sum test showed a lower *FCGBP* level associated with a higher *TP53* mutation rate ( $p = 1.8 \times 10^{-2}$ , Figure 1C). UALCAN analysis on Clinical Proteomic Tumor Analysis Consortium (CTPAC) also pointed out that the *FCGBP* protein levels in tumors ( $n = 108$ ) were lower than those in normal tissues ( $n = 71$ ) ( $p = 2.2 \times 10^{-8}$ , Figure 1D). These findings suggested the downregulation of the *FCGBP* in HNSC tissues at both transcriptional and translational levels.

**Table 1.** Correlations between clinical factors and the *FCGBP* mRNA levels.

Variables	<i>FCGBP</i> mRNA Level		<i>p</i> Value
	Low <i>n</i> = 233	High <i>n</i> = 209	
Gender			1.0
Male	170	152	
Female	63	57	
AJCC <sup>1</sup> T Classification			<0.001
T1/T2	72	99	
T3/T4	161	110	
AJCC <sup>1</sup> N Classification			0.894
N0	106	97	
N1/N2/N3	127	112	
Stage			0.015
Stage I	7	20	
Stage II	33	37	
Stage III	43	38	
Stage IV	150	114	

<sup>1</sup> AJCC: American Joint Committee of Cancer.

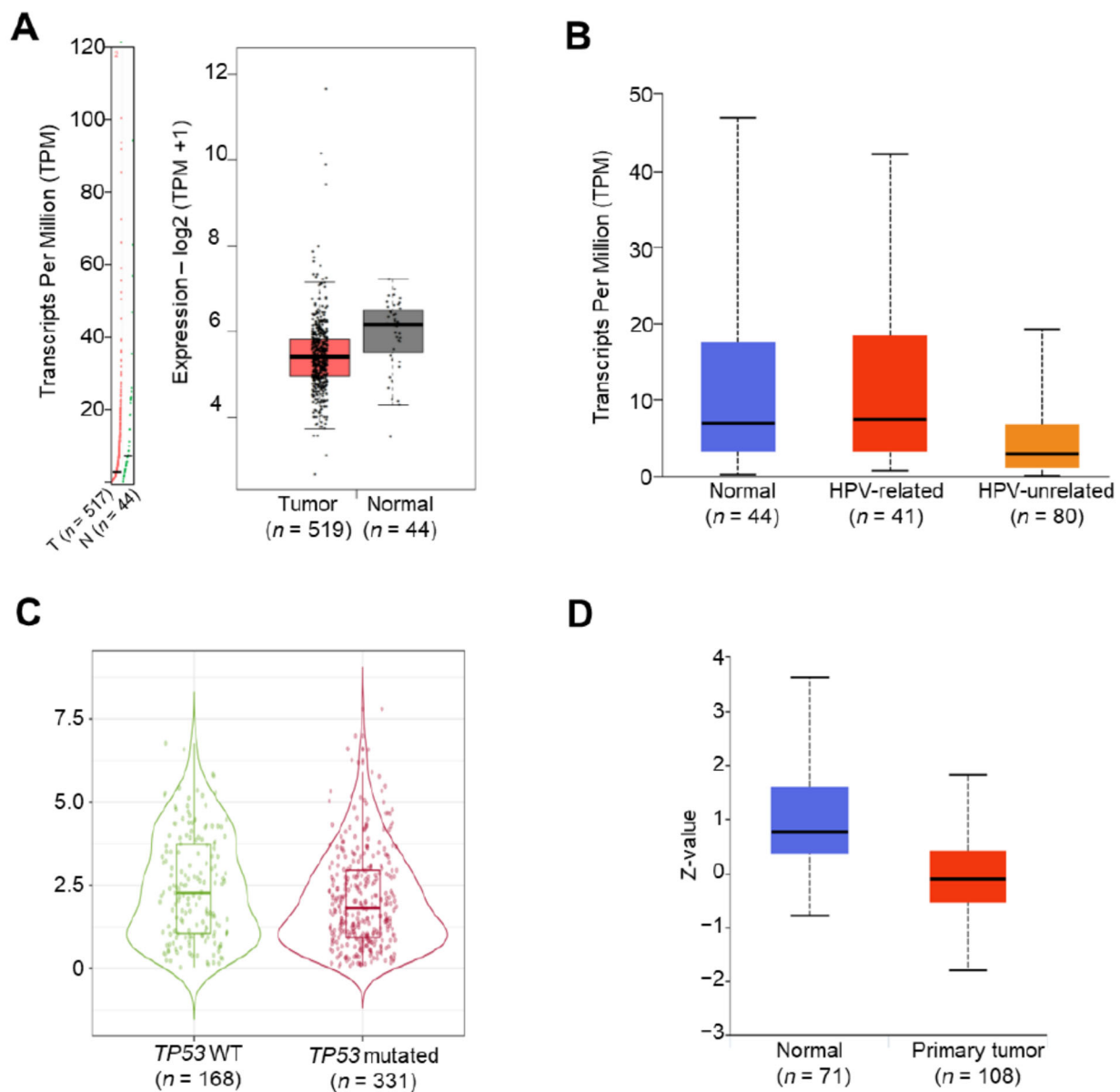


**Figure 1.** The FCGBP levels in head and neck squamous cell carcinoma (HNSC) patients. (A) Gene Expression Profiling Interactive Analysis 2 (GEPIA2) illustrated the differential expression levels of the FCGBP transcript in tumor and adjacent normal tissues based on HNSC dataset. (B) UALCAN showed the FCGBP levels in normal tissues, HPV-related ( $n = 41$ ) and HPV-unrelated ( $n = 80$ ) HNSC. (C) TIMER 2.0 identified the FCGBP levels in HNSC with TP53 wild-type (WT) and mutated, respectively. (D) The protein level of FCGBP in cancer ( $n = 108$ ) and non-cancerous tissues ( $n = 71$ ) were shown, based on Clinical Proteomic Tumor Analysis Consortium (CPTAC).

### 3.2. High FCGBP Level as an Independent Prognostic Factor for Favorable Survival in HNSC

Figure 2A shows the heat map of survivals on various cancers in the pan-TCGA dataset. For HNSC, the Kaplan-Meier curves demonstrated that patients with high FCGBP levels have better overall survival (OS) (hazard ratio [HR] = 0.51,  $p = 9.8 \times 10^{-7}$ ) and disease-free survival (DFS) (HR = 0.47,  $p = 1.1 \times 10^{-5}$ ) compared to those with low FCGBP levels (Figure 2B,C). The univariate Cox model identified the high FCGBP level ( $p = 2 \times 10^{-3}$ ) as a favorable prognostic factor, and high AJCC N ( $p = 2.4 \times 10^{-2}$ ) classification negatively affected OS (Figure 2D). Multivariate analysis revealed that FCGBP level remained a significant prognostic factor, and the results are consistent in both HPV-related ( $n = 98$ , HR = 0.49,  $p = 1.1 \times 10^{-2}$ ) and HPV-unrelated HNSC ( $n = 422$ , HR = 0.75,  $p = 1.4 \times 10^{-3}$ ).

(Figure 2E). Collectively, the above findings suggested that the *FCGBP* level may serve as a positive and independent prognostic factor in patients with HNSC.

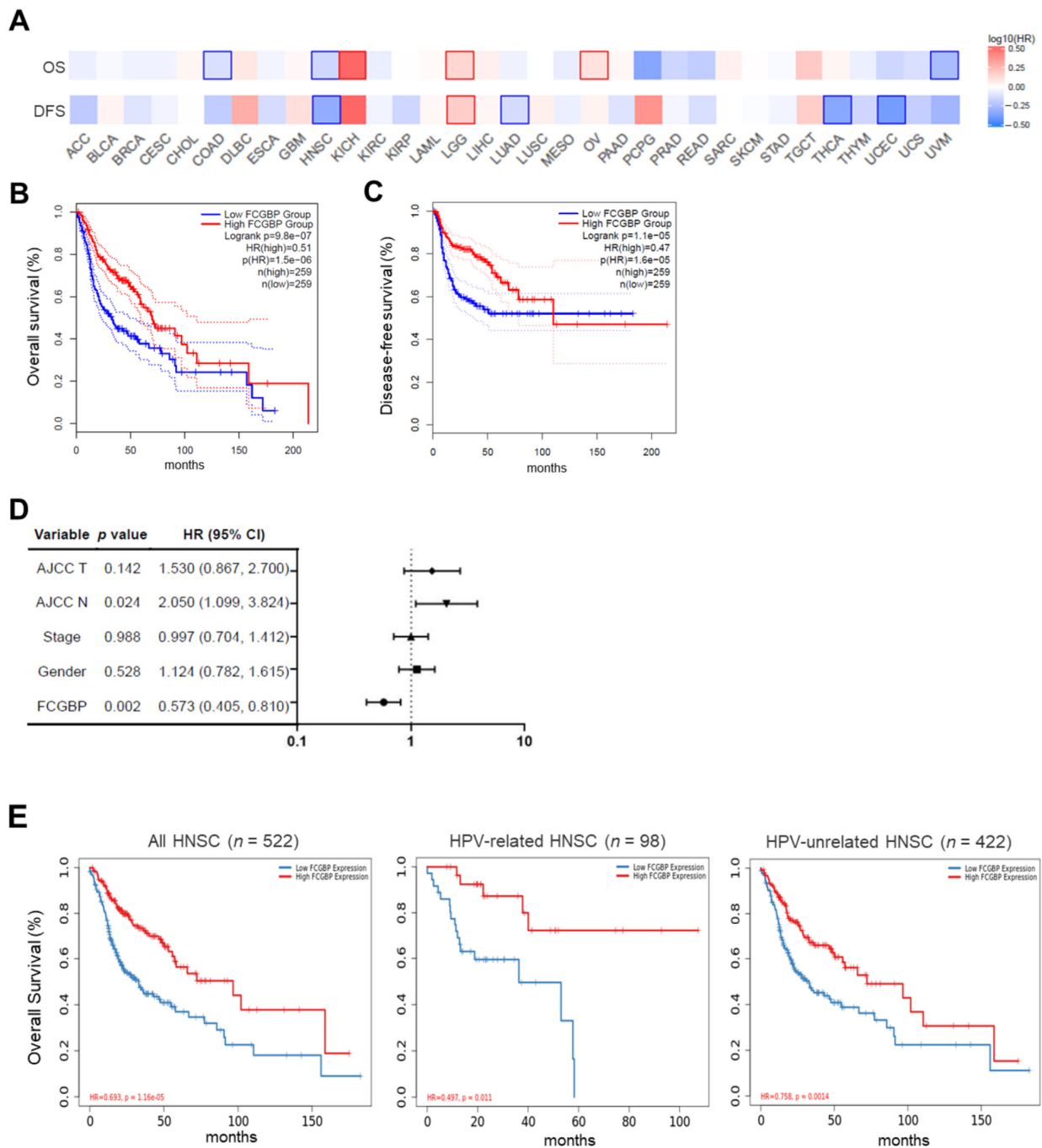


**Figure 2.** Survival analyses of the *FCGBP* level in patients with HNSC. (A) Gene Expression Profiling Interactive Analysis 2 (GEPIA2) illustrated the heat maps of the overall survival (OS) and disease-free survival (DFS) across various cancer types. (B,C) Kaplan–Meier analysis showed OS and DFS of HNSC patients with high *FCGBP* and low *FCGBP* levels based on the GEPIA2. (D) Univariate Cox analysis reveals the hazard ratios (HR) of different variables. (E) Using multivariate analysis, TIMER 2.0 evaluates the OS for all HNSC, HPV-related, and HPV-unrelated HNSC.

### 3.3. The *FCGBP* mRNA Level Positively Correlates to *TP53* WT in HNSC Patients

We analyzed genomic alteration of *FCGBP* in HNSC/TCGA, showing that the alteration rate of the *FCGBP* gene is 6%, with a mutation rate and amplification rate of 4.4% and

0.96%, respectively (Figure 3A). The *FCGBP* gene amplification was negatively associated with its mRNA level in HNSC patients (Figure 3B). Further analysis on the most frequently altered genes, which alternated with the *FCGBP* gene variations, identified *TP53*, *CDKN2A*, *titin (TTN)*, *FAT atypical cadherin 1 (FAT1)*, and *sucrose-isomaltase (SI)*, ranked from high to low in frequency (Figure 3C). Among these genes, *FCGBP* significantly co-occurred with *TP53* ( $q = 3.7 \times 10^{-2}$ ), *SI* ( $q = 1.9E-02$ ), and *FAT1* ( $q = 1.2 \times 10^{-2}$ ) (Supplementary Table S1). Additional examination on the correlation of the *FCGBP* mRNA level and co-occurred genes with TIMER2.0 revealed that *FCGBP* significantly correlated with *TP53* mRNA levels in HNSC patients ( $r = 0.273$ ,  $p = 6.9 \times 10^{-10}$ ) (Figure 3D). Moreover, the *FCGBP* mRNA level was also positively associated with the levels of essential target transcripts of TP53, including *BCL2 binding component 3 (BBC3)* ( $r = 0.169$ ,  $p = 1.64 \times 10^{-4}$ ), *MDM2 proto-oncogene (MDM2)* ( $r = 0.207$ ,  $p = 3.86 \times 10^{-6}$ ), *phorbol-12-myristate-13-acetate-induced protein 1 (PMAIP1)* ( $r = 0.128$ ,  $p = 4.39 \times 10^{-3}$ ), *RNA binding motif protein 10 (RBM10)* ( $r = 0.226$ ,  $p = 4.17 \times 10^{-7}$ ), *zinc finger matrin-type 3 (ZMAT3)* ( $r = 0.292$ ,  $p = 3.68 \times 10^{-11}$ ), and *mutL homolog 1 (MLH1)* ( $r = 0.151$ ,  $p = 7.94 \times 10^{-4}$ ) (Supplementary Figure S1). These findings suggested that a dysregulation of the *FCGBP-TP53* axis potentially participates in the pathogenesis of HNSC.

#### 3.4. The *FCGBP* Correlated with Several Proteins in HNSC Patients

To further explore the interaction between *FCGBP* and potential proteins in HNSC, we used the STRING database and identified 10 proteins that may interact with *FCGBP* (Figure 4A). Intersecting the corresponding genes of the 10 co-expressed proteins with the *FCGBP*-associated co-expressed genes identified by LinkedOmics, four [*TFF3* ( $p = 8.27 \times 10^{-17}$ ), *N-acetylated alpha-linked acidic dipeptidase like 1 (NAALADL1)* ( $p = 6.29 \times 10^{-8}$ ), *zymogen granule protein 16 (G16)* ( $p = 4.72 \times 10^{-3}$ ), and *complement C1q C chain (C1QC)* ( $p = 5.93 \times 10^{-3}$ )] were found with statistical significance (Supplementary Table S2). We next validated these proteins at the mRNA level by TIMER2.0 and found that all of these were significantly correlated to the *FCGBP* level ( $p < 5 \times 10^{-3}$ , Supplementary Table S2).

Notably, *TFF3* ranks at the top one with a significant correlation ( $r = 0.357$ ,  $p = 3.02 \times 10^{-16}$ ) (Figure 4B). *TFF3* closely interact with epidermal growth factor receptor (EGFR, combined score = 0.983) (Supplementary Table S2) through STRING analysis (Supplementary Figure S2A). In addition, *TFF3* downregulation in HNSC tissues, and there is a trend that high-*TFF3* is associated with better OS (Supplementary Figure S2B,C). These findings suggest that *FCGBP* and its co-expression with *TFF3* may collectively contribute to a better survival in HNSC. GeneMania further demonstrated that *FCGBP* co-expressed and co-localized with *TFF3* (Figure 4C). Functional analysis of these differentially expressed transcripts revealed that *FCGBP* may relate to epithelial structure maintenance, protein O-linked glycosylation, and innate immune response (FDR < 0.05, Figure 4C).

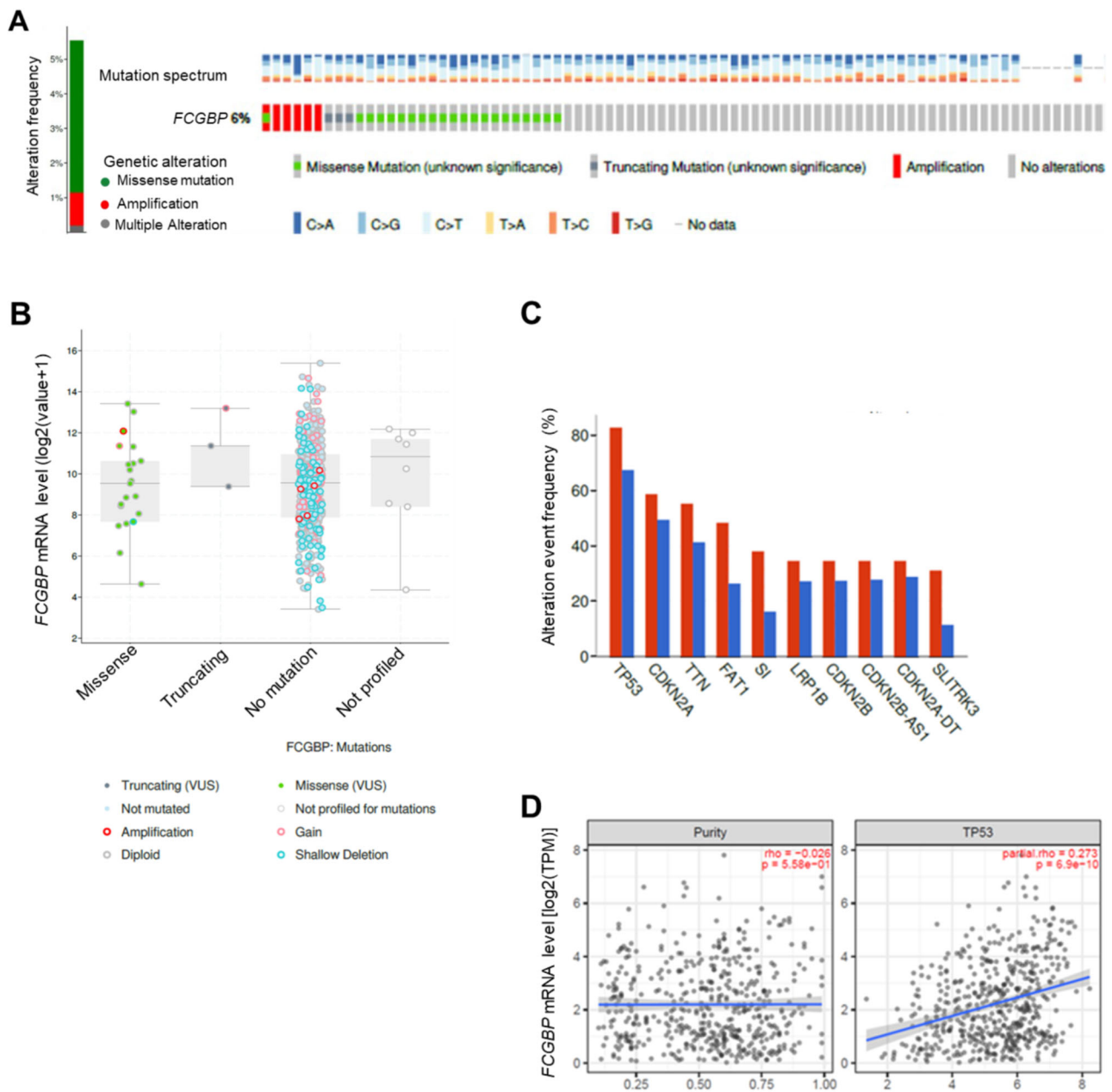


**Figure 3.** Genetic alterations and correlation analysis on the *FCGBP* in HNSC patients. **(A)** cBioPortal showed the *FCGBP* genetic alterations and mutation frequencies. Different colors indicate dissimilar types of genetic alterations. **(B)** The relationships between the *FCGBP* variants and their corresponding mRNA levels (RNA-Seq by Expectation-Maximization: RSEM), batch normalized from Illumina HiSeq\_RANSeqV2. **(C)** The most frequently altered genes with *FCGBP* alteration in HNSC ( $n = 523$ ). **(D)** TIMER2.0 analyzed the correlations between *FCGBP* mRNA level and tumor purity (**left**) and *TP53* mRNA level (**right**).

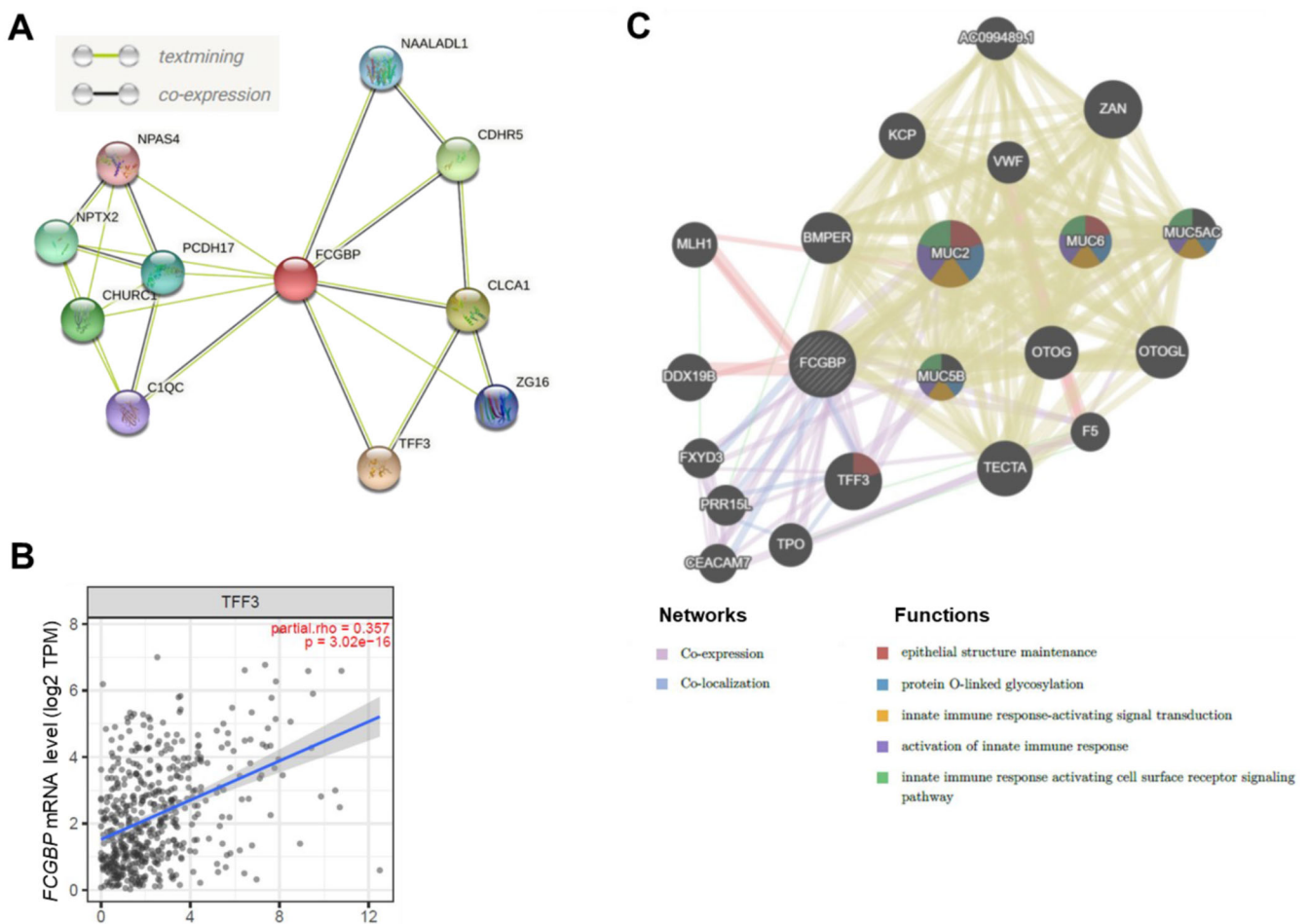


**Figure 4.** The FCGBP interacted gene/protein networks. **(A)** The STRING database showed the FCGBP interacted gene/protein network based on text mining and co-expression. **(B)** TIMER2.0 identified a potential interaction between FCGBP and TFF3 based on co-expression in HNSC patients ( $n = 522$ ; partial  $r = 0.357$ , correlation adjusted by purity;  $p < 0.001$ ). **(C)** The GeneMania database showed the gene-gene interaction network. The association between FCGBP and TFF3 based on co-expression and co-localization highlighted the genes with function enriched in epithelial structure maintenance.

### 3.5. Functional Enrichment Analysis of FCGBP and Co-Expressed Genes in HNSC

To explore the potential functions and pathways of FCGBP in HNSC, we identified a total of 10,116 significantly correlated genes by the LinkedOmics database shown in volcano plot ( $p < 0.01$  and  $FDR < 0.01$ , Figure 5A). Figure 5B shows the top 50 genes which were positively correlated to the FCGBP level. Further functional enrichment of biologic process (Figure 5C) of the GO analysis revealed that the GO function of the co-expressed genes is shown as enriched bar diagrams. The most significant enriched GO term at the biologic process level was ‘alpha-beta T cell differentiation (enrichment ratio = 2.29)’ (Figure 5C). Other GO terms include ‘immune response-activating signal transduction (enrichment ratio = 1.66)’, ‘regulation of lymphocyte activation (enrichment ratio = 1.62)’, and ‘regulation of immune response (enrichment ratio = 1.54)’ ( $p < 0.05$  and  $FDR < 0.05$ , Figure 5C). Further GSEA on KEGG pathways showed that the enrichment terms of these co-expressed genes are predominantly involved in immune and inflammatory responses, including ‘Th17 cell differentiation’, ‘T cell receptor signaling pathways’, ‘cytokine-cytokine receptor interaction’, and ‘chemokine signaling pathway’, indicating that the FCGBP may be an immune-related factor in HNSC ( $FDR < 0.05$ , Figure 5D).

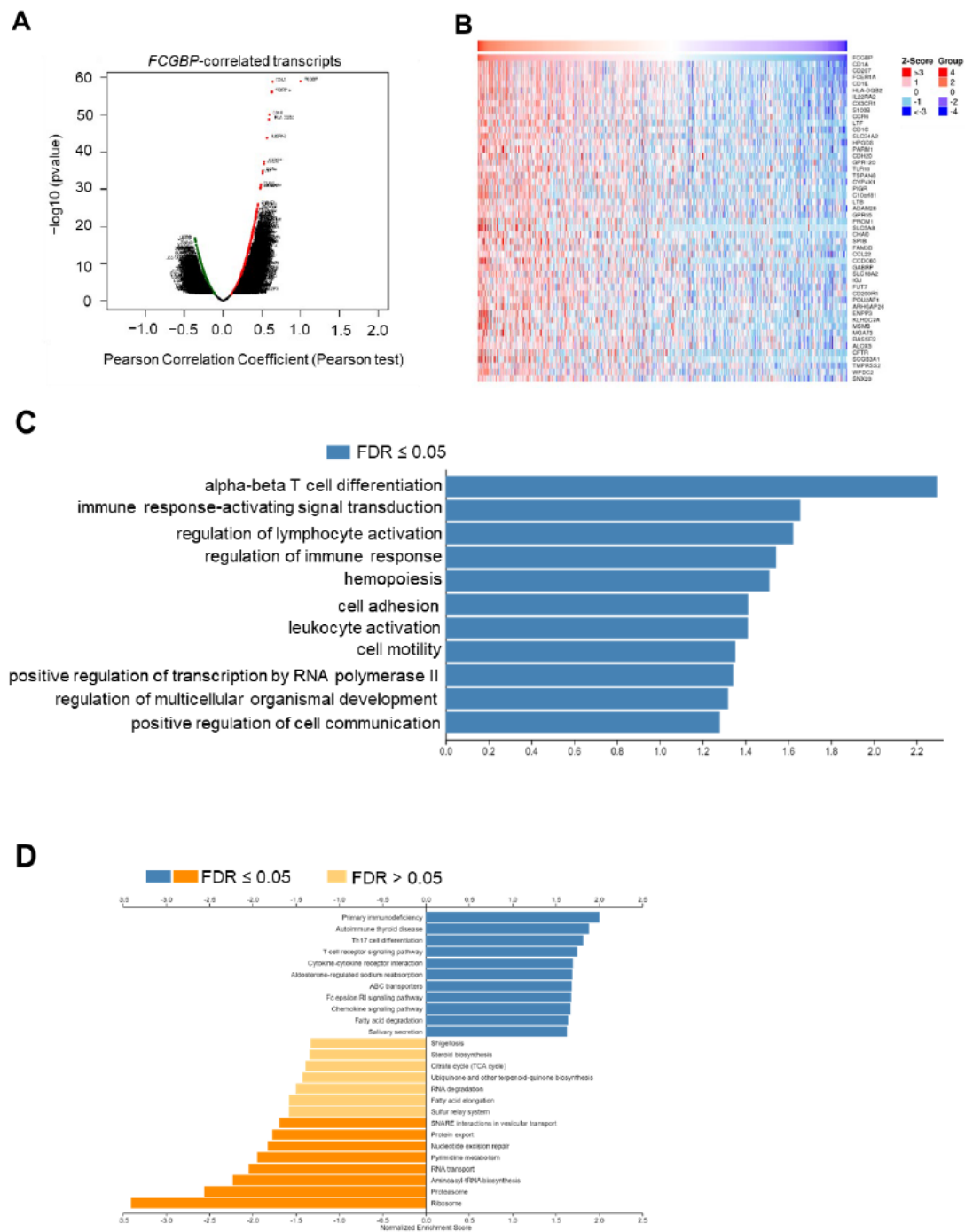


**Figure 5.** The FCGBP-correlated transcripts and enrichment analysis. **(A)** LinkedOmics showed the volcano map of 20,163 FCGBP co-expressed transcripts in 517 HNSCs by the Pearson correlation analysis (red: positive; green: negative). **(B)** The heat maps displayed the top 50 transcripts positively correlated to the FCGBP level. **(C)** The bar diagram demonstrated the co-expressed transcripts with significantly enriched GO (Biological Process) annotations ( $p < 0.05$  and FDR < 0.05). **(D)** Gene Set Enrichment Analysis (GSEA) showed the enriched KEGG pathways (FDR < 0.05).

### 3.6. The FCGBP Level Correlates to Immunomodulators and Immune-Related Molecules, and the Abundance of Infiltration of Immune Cells

We evaluated the association of the FCGBP level and immunomodulators on the TISIDB database. The FCGBP levels positively correlated to immunostimulators across various tumors (Figure 6A). In 522 HNSC, the FCGBP level positively correlated to most



( $r = -1$  to  $+1$ ) between various immunostimulators and the HNSC (arrow) among distinct cancer types. (B) In HNSC patients ( $n = 522$ , TCGA), the correlations ( $r$ ) between the *FCGBP* level and the *CD27*, *TNFRSF13B*, *ICOSLG*, and *TNFRSF17* levels, respectively. (C) Heat maps indicated the correlations ( $r = -1$  to  $+1$ ) between various infiltration immune cells and the HNSC (arrow) among distinct cancer types. (D) In HNSC 522 patients (TCGA), the correlations ( $r$ ) between the *FCGBP* level and abundance of effector memory CD8 T cell (Tem\_CD8), type 17 helper cell (Th17), T follicular helper cells (*Tfh*), activated B cells (Act\_B), and mast cells (Mast). (E,F) Heat maps of chemokines, chemokine receptors and the HNSC (arrow) among distinct cancer types.

We next performed a comprehensive screening on the infiltration of immune cells using the TISIDB database (Figure 6C). TIMER2.0 identified the meaningful infiltrated immune cells in the same directions with different algorithms. The *FCGBP* level correlated with infiltration rates of effector memory CD8+ T cells (Tem\_CD8+,  $r = 0.274$ ,  $p = 2.2 \times 10^{-10}$ ), Type 17 helper cells (Th17,  $r = 0.328$ ,  $p = 1.82 \times 10^{-14}$ ), T follicular helper cells (Tfh,  $r = 0.164$ ,  $p = 1.66 \times 10^{-4}$ ), activated B cells (Act\_B,  $r = 0.382$ ,  $p < 2.2 \times 10^{-16}$ ), and mast cells (Mast,  $r = 0.172$ ,  $p = 7.81 \times 10^{-5}$ ) (Figure 6D). To additionally strengthen the role of *FCGBP* in identified immune cells, we explored the association between the *FCGBP* level and the respective immune markers. Most markers were strongly associated with the *FCGBP* level in HNSC (Table 2), suggesting that *FCGBP* was strongly associated with tumor-infiltrating immune cells in HNSC. Moreover, consistent survival trends for the *FCGBP* level and involving immune cells existed. The survivals of patients with low infiltration immune cells were worse than those with high infiltration (Supplementary Figure S3).

Further TISIDB analysis on the correlations between the *FCGBP* level, chemokines, and receptors showed that *FCGBP* might regulate various immune molecules (Figure 6E,F). The top two molecules and receptors with high correlations were *C-C motif chemokine ligand 22* (*CCL22*) and *CCL19*, and *C-C motif chemokine receptor 6* (*CCR6*) and *C-X3-C motif chemokine receptor 1* (*CX3CR1*), respectively. These findings further suggest that *FCGBP* and its co-expressed genes may participate in the immune response of the HNSC tumor microenvironment. In addition, we verified the relationship between *FCGBP* and immune checkpoints, which revealed that the *FCGBP* level positively associated with those of *CTLA4* ( $r = 0.295$ ,  $p = 2.56 \times 10^{-11}$ ), *HAVCR2* ( $r = 0.225$ ,  $p = 4.41 \times 10^{-7}$ ), *LAG3* ( $r = 0.162$ ,  $p = 3.1 \times 10^{-4}$ ), *PDCD1* ( $r = 0.303$ ,  $p = 6.95 \times 10^{-12}$ ) (Table 2). The differential expression levels of various immune checkpoints with *FCGBP* expression may suggest the use of immunotherapy.

**Table 2.** Associations between FCGBP level and gene markers in tumor-infiltrating immune cells in HNSC by HPV infection status.

Cell Type	Marker	<sup>1</sup> HNSC (n = 522)				<sup>2</sup> HPV-Unrelated HNSC (n = 422)				HPV-Related HNSC (n = 98)			
		<sup>3</sup> Purity		<sup>4</sup> None		Purity		None		Purity		None	
		<sup>5</sup> Correlation	p Value	Correlation	p Value	Correlation	p Value	Correlation	p Value	Correlation	p Value	Correlation	p Value
B	CD19	0.38	***	0.38	***	0.32	***	0.33	***	0.37	***	0.32	**
	CD79A	0.42	***	0.41	***	0.35	***	0.36	***	0.43	***	0.37	***
	CD86	0.19	***	0.20	***	0.18	***	0.19	***	0.19	7.13 × 10 <sup>-2</sup>	0.15	1.33 × 10 <sup>-1</sup>
	CSF1R	0.34	***	0.33	***	0.32	***	0.31	***	0.38	***	0.33	**
Plasma	CD38	0.11	*	0.13	**	0.08	1.12 × 10 <sup>-1</sup>	0.09	6.82 × 10 <sup>-2</sup>	0.23	*	0.13	**
	CXCR4	0.31	***	0.32	***	0.26	***	0.27	***	0.34	**	0.35	***
	TNFRSF17	0.37	***	0.37	***	0.31	***	0.32	***	0.39	***	0.34	***
	CD27	0.41	***	0.40	***	0.35	***	0.35	***	0.44	***	0.38	***
CD8+ T	CD8A	0.28	***	0.29	***	0.21	***	0.23	***	0.38	***	0.35	***
	CD8B	0.28	***	0.29	***	0.20	***	0.22	***	0.40	***	0.41	***
Follicular helper T	IL21	0.23	***	0.24	***	0.16	**	0.18	***	0.34	**	0.32	**
	BCL6	0.30	***	0.28	***	0.29	***	0.26	***	0.25	1.71 × 10 <sup>-2</sup>	0.22	*
	ICOS	0.29	***	0.29	***	0.25	***	0.26	***	0.32	**	0.32	**
	CXCR5	0.42	***	0.41	***	0.38	***	0.38	***	0.37	***	0.33	***
Th17	STAT3	0.37	***	0.37	***	0.32	***	0.31	***	0.50	***	0.49	***
	IL-17A	0.34	***	0.34	***	0.26	***	0.28	***	0.49	***	1.74	***
	IL-21R	0.41	***	0.40	***	0.35	***	0.35	***	0.48	***	1.47	***
	IL-23R	0.31	***	0.31	***	0.27	***	0.27	***	0.38	***	0.39	***
T cell exhaustion	PDCD1	0.30	***	0.31	***	0.22	***	0.24	***	0.42	***	0.39	***
	CTLA4	0.30	***	0.30	***	0.23	***	0.25	***	0.40	***	0.39	***
	LAG3	0.16	***	0.17	***	0.09	6.85 × 10 <sup>-2</sup>	0.11	*	0.29	**	0.28	**
	HAVCR2	0.23	***	0.22	***	0.18	***	0.19	***	0.29	**	0.23	*

<sup>1</sup> HNSC: head and neck squamous cell carcinoma, <sup>2</sup> HPV: human papillomavirus, <sup>3</sup> Purity: correlation adjusted by tumor purity; <sup>4</sup> None: correlation without adjustment; <sup>5</sup> Correlation: R value of Spearman's correlation. \* p < 0.05, \*\* p < 0.01, \*\*\* p < 0.001.

#### 4. Discussion

This study found that the FCGBP can be used as an independent prognostic factor in head and neck squamous cell carcinoma, regardless of the HPV infection status. One of the potential mechanisms underlying the association of low-FCGBP with poor prognosis was downregulated FCGBP correlated to a higher TP53 mutation rate. Moreover, FCGBP correlates to TFF3, a prognostic biomarker in various cancers, at transcriptional and translational levels. An additional reason for the predictive value of FCGBP is its ability to regulate the immune responses of the HNSC tumor microenvironment, since FCGBP associated co-expressed genes were predominantly enriched in immune responses. Further, FCGBP mRNA level was significantly associated with those of various immune stimulators and immune molecules and regulated the infiltration rates of immune cells.

The potential roles of *FCGBP* in cancer initiation, progression, and prognoses have been proposed in certain malignancies. *FCGBP* represents the most under-expressed gene in the TGF- $\beta$ -induced gallbladder carcinoma-derived cells compared to a normal cell line, suggesting its role in TGF $\beta$ -induced EMT to drive metastatic behaviors [16]. However, high FCGBP protein levels in human specimens correlated to increased incidence of metastasis and better OS [16]. Moreover, the FCGBP protein levels in colorectal cancer, were lower in metastatic tissues than in the paired primary tumors, and validated as an independent prognostic factor for metastatic colon cancer [17]. In HNSC, immunohistochemistry demonstrated that the FCGBP protein levels were lower in cancer tissues than noncancerous tissues retrieved from the surgical margin [19]. Similarly, the *FCGBP* level in cancer tissues is higher in HPV-related than HPV-unrelated HNSC, and these findings are consistent with the prediction by the CTPAC analysis. Further functional analysis validated the effects of *FCGBP* on HNSC behaviors, whereas its overexpression in FaDu cells and Cal-27 cells decreased proliferation and inhibited EMT. Moreover, both mRNA and protein levels of TGF $\beta$  were negatively correlated to *FCGBP*, and further evidence indicates that *FCGBP* level decreased by TGF $\beta$  treatment and increased by E6 overexpression, suggesting that upregulated *FCGBP* may contribute to suppression of HNSC [19].

*TP53* may play a role in the pathogenesis of *FCGBP* in HNSC; our results showed that *TP53* was the most frequently altered gene with *FCGBP* alteration, and the tendency for the co-occurred alterations of *TP53* and *FCGBP* is significant. Further evidence strengthened the correlation between *FCGBP* and *TP53* was a significant correlation between *FCGBP* and *TP53* targeted genes, including *BBC3*, *MDM2*, *PMAIP1*, *RBM10*, *ZMAT3* and *MLH1*. *TP53* primarily acts as a tumor suppressor in head and neck cancer. Recent studies have pointed out that, in addition to controlling various cellular processes (e.g., apoptosis, cell cycle, senescence) in response to cellular stress to antagonized malignant progression [31], the *TP53*-mediated tumor suppression also involved activation of ferroptosis [32], remodeling cancer metabolism [33], inhibition of cellular self-renewal [34], ensuring genomic integrity [35], and maintenance a tumor-suppressive immune response [36]. *TP53* may also modulate a target gene network to suppress tumorigenesis [35,37]. Through in vivo shRNA and CRISPR/Cas9 screens, the tumor suppressors *ZMAT3* [35,37] and *MLH1* [35] were identified as predominant *TP53* target effectors to the *TP53*-mediated tumor suppression program. In our correlation analysis, the *FCGBP* level positively associated with *ZMAT3* and *MLH1* irrespective of the HPV status, and these findings may partially explain the inverse relationships of *FCGBP* level with AJCC T classification and AJCC stage from the perspective of the role of *TP53* in HNSC.

Current bioinformatics analysis demonstrated an inverse relationship between *TP53* mutation, the most frequently mutated gene (69.3%) in HNSC in the Pan-Cancer Atlas (TCGA), and the *FCGBP* level. The majority of *TP53* mutations are missense mutations, and the most common *TP53* mutations occur mainly in the DNA-binding domain to affect DNA binding residues or cause conformational change to prevent DNA binding [38]. The consequence includes the loss of the transcriptional function of wild-type (WT) *TP53*, dominant-negative activity that mutant *TP53* suppresses the ability of WT *TP53*, and/or gain-of-function that mutant *TP53* acquire oncogenic activities independently of

WT TP53 [38]. Despite *TP53* mutation not necessarily causing attenuation of TP53 activity, a genomic investigation of the TCGA consisting of 279 HNSC patients identified the most significant mutations leading to TP53 inactivation were *TP53* (84%) and *CDKN2A* (57%) in HPV-unrelated HNSC [39]. Of interest, the study identified a subgroup of oral cavity cancer patients with favorable outcomes characterized by reduced copy number alteration in conjugation with inactivating *CASP8* mutations and WT *TP53* [39]. Further computational analysis of 415 HNSC patients in TCGA otherwise demonstrated *TP53* mutation is an independent prognostic factor for reduced overall survival, although the impact is affected by the types of mutations and the localization of the mutation within *TP53* [40]. More specific analyses on the transactivation activity of mutant TP53 showing the nonfunctional *TP53* mutation is indicative of reduced response to cisplatin and fluorouracil [41]. Accordingly, these findings may suggest that *FCGBP* downregulation in HNSC predicted worse survivals to a certain extent, especially in the HPV-unrelated HNSC since *TP53* is rarely altered in HPV-related HNSC [39].

Another possible mechanism for low *FCGBP* as an inferior prognostic factor in HNSC is *TFF3* might interact with *FCGBP*. In the genetic network analysis, *FCGBP* and *TFF3* are co-expressed and co-localized, revealing their associations at transcriptional and translational levels. *TFF3* is a secretory lectin and represents the predominant TFF peptide of human saliva and esophageal secretions [42,43]. Physiologically, *TFF3* may bind *FCGBP* to form a heterodimer to protect the mucosa by reinforcing innate immunity [9,44]. Interestingly, *TFF3* has multifaceted effects from a pre-neoplastic lesion to invasive cancer, and the roles in several cancer subtypes have been extensively discussed [45–47]. In colorectal cancer, *TFF3* promotes proliferation, invasion, and migration by enhancing CD147–CD44 interaction to activate transcription 3 (STAT3) and prostaglandin G/H synthase 2 (PTGS2) expression [46]. In prostate cancer, *TFF3* silencing induced mitochondria-mediated apoptosis, thus suppressing tumor growth and migration [47]. The roles of *TFF3* in promoting tumor progression were also well established in breast, cervical, hepatocellular, and gastric cancers and glioblastoma. However, *TFF3* contrarily acts as a tumor suppressor in retinoblastoma [45]. Since protein–protein interaction is essential in the molecular mechanisms underlying carcinogenesis and cancer progression and aggressiveness, aberrant *FCGBP* expression may regulate cancer behaviors by functional interactome linking with *TFF3*. Our results may potentially rationalize the assumption because *TFF3* level, such as *FCGBP* expression, was reduced in HNSC tissue, and survival decreased in patients with HNSC of downregulated *TFF3*. Another supporting finding is that *FCGBP* in thyroid cancer can functionally synergize with *TFF3* through genetic co-expression, and thus contributing to poor survival in thyroid cancer patients with low *TFF3* level [48].

In addition, *FCGBP* may participate in the immune response in the tumor microenvironment of HNSC. Our GO analysis results demonstrated that the *FCGBP*-associated co-expressed genes were primarily enriched in immune and inflammatory responses, including ‘regulation of lymphocyte activation’, ‘regulation of immune response’, and ‘immune response-activating signal transduction’ for GO at the biological process level. Our GSEA results of the KEGG pathway also revealed that the enriched terms are predominantly related to the immune process, including ‘T cell receptor signaling pathways’, ‘cytokine–cytokine receptor interaction’, and ‘chemokine signaling pathways’. Altogether, these findings imply that *FCGBP* levels may be related to the immune interaction with HNSC. *FCGBP* may be involved in the tumor microenvironment of HNSC to regulate cancer development because cytokines and chemokines are critical noncellular components of the tumor microenvironment [49].

Further exploration of the association of *FCGBP* expression with diverse immune molecules and immune-stimulator genes may support the assumption that most of them are significantly correlated to *FCGBP* level. Thus, we analyzed the composition of tumor-infiltrating immune cells correlating to *FCGBP* levels in HNSC samples. The *FCGBP* level was positively associated with infiltration rates of CD8+ T-cell, T17 lymphocyte, B-cell, mast cell, and follicular helper T-cell. The correlation was strengthened with the strong

associations of the FCGBP level with those of most of these cells' type-specific markers irrespective of the HPV infection status. Previous investigations have pointed out that the dense infiltration of the CD8+ T cells within tumor microenvironment confers a favorable prognosis for its antitumor property [50,51], we hypothesized that a low FCGBP level in the tumor tissue might shape the tumor microenvironment in an immune-suppressed state. There is a consistent survival trend between the FCGBP level and immune cell abundance, i.e., the survival is worse in low-abundant immune cells. Consequently, the predictive value of FCGBP, at least, might result from better immune control from the perspective of immune infiltration.

This study has some limitations. First, the study used heterogeneous datasets in different databases; therefore, the analysis by the other platforms may produce inconsistent results. Except for GeneMania and STRING, all other studies used available data from TCGA with different platforms. Because the required raw data for each analysis may be unavailable in the cohort, the total number of HNSC recruited differs by different analyses. Nonetheless, despite the slight difference in recruited samples in each analysis, the overall trend for FCGBP was present. For example, FCGBP was an independent prognostic factor for both HPV-related and HPV-unrelated HNSCs since the HPV status may cause a distinct difference in cancer behaviors of HNSC. Second, although other datasets have validated the findings of TCGA; the results should be extrapolated cautiously to non-primary ethnicities. Third, we explored the role of FCGBP in HNSC from a survival perspective, the effects of chemotherapy and radiation therapy cannot be ignored. Although we can forecast drug sensitivity from bioinformatics prediction, the complexity of treatment, for example, treatment intensity or treatment sequence may make us overestimate or underestimate the role of FCGBP. Future experiments focusing on validating the present predictions are warranted to improve the value of FCGBP application in HNSC.

## 5. Conclusions

Taken together, FCGBP level was significantly reduced in HNSC tissues, and a high-FCGBP level indicated favorable prognoses. Further analyses demonstrated that FCGBP alteration significantly co-occurred with that of TP53, and FCGBP levels were negatively associated with the TP53 mutation rate. Additionally, FCGBP might interact with TFF3, an essential protein in the pathogenesis of several cancers. With the finding that FCGBP level significantly correlates with infiltration rates of various immune cells and expression levels of immune molecules to possibly regulate the immune response of the tumor microenvironment, FCGBP may be a potential prognostic biomarker in head and neck squamous cell carcinoma. However, further studies are needed to clarify these.

**Supplementary Materials:** The following are available online at <https://www.mdpi.com/article/10.3390/diagnostics12051178/s1>, Table S1. Correlations between FCGBP alterations and top altered genes in HNSC patients ( $n = 522$ ). Table S2. Intersection analysis of interacted proteins with FCGBP and FCGBP-associated co-expressed genes. Figure S1. The correlations between FCGBP and the target genes of TP53. Figure S2. The interacting network, expression levels, and survival analysis of TFF3. Figure S3. Survival analyses by high- and low- levels of FCGBP and infiltration rates of immune cells.

**Author Contributions:** Conception and design: Y.-H.L., Y.-F.Y., Y.-L.S. Collection and assembly of data: Y.-H.L., Y.-F.Y., Y.-L.S. Data analysis and interpretation: Y.-H.L., Y.-F.Y., Y.-L.S. Manuscript writing: Y.-H.L., Y.-L.S. Final approval of manuscript: Y.-H.L., Y.-F.Y., Y.-L.S. All authors have read and agreed to the published version of the manuscript.

**Funding:** This study was supported by grants from the Ministry of Science and Technology, Taipei, Taiwan (MOST-110-2314-B-075B-014).

**Institutional Review Board Statement:** The protocol of this study was approved by the institutional review board of Kaohsiung Veterans General Hospital.

**Informed Consent Statement:** Not applicable.

**Data Availability Statement:** The data presented in this study are available on request from the corresponding author.

**Conflicts of Interest:** The authors declare no conflict of interest.

## References

1. Bray, F.; Ferlay, J.; Soerjomataram, I.; Siegel, R.L.; Torre, L.A.; Jemal, A. Global cancer statistics 2018: GLOBOCAN estimates of incidence and mortality worldwide for 36 cancers in 185 countries. *CA Cancer J. Clin.* **2018**, *68*, 394–424. [[CrossRef](#)] [[PubMed](#)]
2. D'Souza, G.; Westra, W.H.; Wang, S.J.; van Zante, A.; Wentz, A.; Kluz, N.; Rettig, E.; Ryan, W.R.; Ha, P.K.; Kang, H.; et al. Differences in the Prevalence of Human Papillomavirus (HPV) in Head and Neck Squamous Cell Cancers by Sex, Race, Anatomic Tumor Site, and HPV Detection Method. *JAMA Oncol.* **2017**, *3*, 169–177. [[CrossRef](#)] [[PubMed](#)]
3. Grulich, A.E.; Jin, F.; Conway, E.L.; Stein, A.N.; Hocking, J. Cancers attributable to human papillomavirus infection. *Sex. Health* **2010**, *7*, 244–252. [[CrossRef](#)] [[PubMed](#)]
4. Wiest, T.; Schwarz, E.; Enders, C.; Flechtenmacher, C.; Bosch, F.X. Involvement of intact HPV16 E6/E7 gene expression in head and neck cancers with unaltered p53 status and perturbed pRb cell cycle control. *Oncogene* **2002**, *21*, 1510–1517. [[CrossRef](#)]
5. Rettig, E.M.; D'Souza, G. Epidemiology of head and neck cancer. *Surg. Oncol. Clin. N. Am.* **2015**, *24*, 379–396. [[CrossRef](#)]
6. Kobayashi, K.; Ogata, H.; Morikawa, M.; Iijima, S.; Harada, N.; Yoshida, T.; Brown, W.R.; Inoue, N.; Hamada, Y.; Ishii, H.; et al. Distribution and partial characterisation of IgG Fc binding protein in various mucin producing cells and body fluids. *Gut* **2002**, *51*, 169–176. [[CrossRef](#)]
7. Denny, P.; Hagen, F.K.; Hardt, M.; Liao, L.; Yan, W.; Arellanno, M.; Bassilian, S.; Bedi, G.S.; Boonthueung, P.; Cociorva, D.; et al. The proteomes of human parotid and submandibular/sublingual gland salivas collected as the ductal secretions. *J. Proteome Res.* **2008**, *7*, 1994–2006. [[CrossRef](#)]
8. Li, C.; Wang, R.; Su, B.; Luo, Y.; Terhune, J.; Beck, B.; Peatman, E. Evasion of mucosal defenses during *Aeromonas hydrophila* infection of channel catfish (*Ictalurus punctatus*) skin. *Dev. Comp. Immunol.* **2013**, *39*, 447–455. [[CrossRef](#)]
9. Albert, T.K.; Laubinger, W.; Müller, S.; Hanisch, F.G.; Kalinski, T.; Meyer, F.; Hoffmann, W. Human intestinal TFF3 forms disulfide-linked heteromers with the Mucus-Associated FCGBP protein and is released by hydrogen sulfide. *J. Proteome Res.* **2010**, *9*, 3108–3117. [[CrossRef](#)]
10. Kim, M.; Lee, S.; Yang, S.K.; Song, K.; Lee, I. Differential expression in histologically normal crypts of ulcerative colitis suggests primary crypt disorder. *Oncol. Rep.* **2006**, *16*, 663–670. [[CrossRef](#)]
11. Risques, R.A.; Lai, L.A.; Himmetoglu, C.; Ebaee, A.; Li, L.; Feng, Z.; Bronner, M.P.; Al-Lahham, B.; Kowdley, K.V.; Lindor, K.D.; et al. Ulcerative colitis-associated colorectal cancer arises in a field of short telomeres, senescence, and inflammation. *Cancer Res.* **2011**, *71*, 1669–1679. [[CrossRef](#)] [[PubMed](#)]
12. Zhou, C.; Chen, H.; Han, L.; Xue, F.; Wang, A.; Liang, Y.J. Screening of genes related to lung cancer caused by smoking with RNA-Seq. *Eur. Rev. Med. Pharmacol. Sci.* **2014**, *18*, 117–125. [[PubMed](#)]
13. Wang, A.; Wu, L.; Lin, J.; Han, L.; Bian, J.; Wu, Y.; Robson, S.C.; Xue, L.; Ge, Y.; Sang, X.; et al. Whole-exome sequencing reveals the origin and evolution of hepato-cholangiocarcinoma. *Nat. Commun.* **2018**, *9*, 894. [[CrossRef](#)] [[PubMed](#)]
14. Gazi, M.H.; He, M.; Chevillat, J.C.; Young, C.Y. Downregulation of IgG Fc binding protein (Fc gammaBP) in prostate cancer. *Cancer Biol. Ther.* **2008**, *7*, 70–75. [[CrossRef](#)]
15. O'Donovan, N.; Fischer, A.; Abdo, E.M.; Simon, F.; Peter, H.J.; Gerber, H.; Buergi, U.; Marti, U. Differential expression of IgG Fc binding protein (Fc gammaBP) in human normal thyroid tissue, thyroid adenomas and thyroid carcinomas. *J. Endocrinol.* **2002**, *174*, 517–524. [[CrossRef](#)] [[PubMed](#)]
16. Xiong, L.; Wen, Y.; Miao, X.; Yang, Z. NT5E and FcGBP as key regulators of TGF-1-induced epithelial-mesenchymal transition (EMT) are associated with tumor progression and survival of patients with gallbladder cancer. *Cell Tissue Res.* **2014**, *355*, 365–374. [[CrossRef](#)] [[PubMed](#)]
17. Yuan, Z.; Zhao, Z.; Hu, H.; Zhu, Y.; Zhang, W.; Tang, Q.; Huang, R.; Gao, F.; Zou, C.; Wang, G.; et al. IgG Fc Binding Protein (FCGBP) is Down-Regulated in Metastatic Lesions and Predicts Survival in Metastatic Colorectal Cancer Patients. *Oncotargets Ther.* **2021**, *14*, 967–977. [[CrossRef](#)]
18. Choi, C.H.; Choi, J.J.; Park, Y.A.; Lee, Y.Y.; Song, S.Y.; Sung, C.O.; Song, T.; Kim, M.K.; Kim, T.J.; Lee, J.W.; et al. Identification of differentially expressed genes according to chemosensitivity in advanced ovarian serous adenocarcinomas: Expression of GRIA2 predicts better survival. *Br. J. Cancer* **2012**, *107*, 91–99. [[CrossRef](#)]
19. Wang, Y.; Liu, Y.; Liu, H.; Zhang, Q.; Song, H.; Tang, J.; Fu, J.; Wang, X. FcGBP was upregulated by HPV infection and correlated to longer survival time of HNSCC patients. *Oncotarget* **2017**, *8*, 86503–86514. [[CrossRef](#)]
20. Chen, S.M.Y.; Krinsky, A.L.; Woolaver, R.A.; Wang, X.; Chen, Z.; Wang, J.H. Tumor immune microenvironment in head and neck cancers. *Mol. Carcinog.* **2020**, *59*, 766–774. [[CrossRef](#)]
21. Chow, L.Q.M.; Haddad, R.; Gupta, S.; Mahipal, A.; Mehra, R.; Tahara, M.; Berger, R.; Eder, J.P.; Burtneess, B.; Lee, S.H.; et al. Antitumor Activity of Pembrolizumab in Biomarker-Unselected Patients with Recurrent and/or Metastatic Head and Neck Squamous Cell Carcinoma: Results from the Phase Ib KEYNOTE-012 Expansion Cohort. *J. Clin. Oncol.* **2016**, *34*, 3838–3845. [[CrossRef](#)] [[PubMed](#)]

22. Tang, Z.; Kang, B.; Li, C.; Chen, T.; Zhang, Z. GEPIA2: An enhanced web server for large-scale expression profiling and interactive analysis. *Nucleic Acids Res.* **2019**, *47*, W556–W560. [[CrossRef](#)] [[PubMed](#)]
23. Li, T.; Fan, J.; Wang, B.; Traugh, N.; Chen, Q.; Liu, J.S.; Li, B.; Liu, X.S. TIMER: A Web Server for Comprehensive Analysis of Tumor-Infiltrating Immune Cells. *Cancer Res.* **2017**, *77*, e108–e110. [[CrossRef](#)] [[PubMed](#)]
24. Chandrashekar, D.S.; Bashel, B.; Balasubramanya, S.A.H.; Creighton, C.J.; Rodriguez, I.P.; Chakravarthi, B.V.S.K.; Varambally, S. UALCAN: A portal for facilitating tumor subgroup gene expression and survival analyses. *Neoplasia* **2017**, *19*, 649–658. [[CrossRef](#)]
25. Chen, F.; Chandrashekar, D.S.; Varambally, S.; Creighton, C.J. Pan-cancer molecular subtypes revealed by mass-spectrometry-based proteomic characterization of more than 500 human cancers. *Nat. Commun.* **2019**, *10*, 5679. [[CrossRef](#)]
26. Cerami, E.; Gao, J.; Dogrusoz, U.; Gross, B.E.; Sumer, S.O.; Aksoy, B.A.; Jacobsen, A.; Byrne, C.J.; Heuer, M.L.; Larsson, E.; et al. The cBio cancer genomics portal: An open platform for exploring multidimensional cancer genomics data. *Cancer Discov.* **2012**, *2*, 401–404. [[CrossRef](#)]
27. Szklarczyk, D.; Gable, A.L.; Lyon, D.; Junge, A.; Wyder, S.; Huerta-Cepas, J.; Simonovic, M.; Doncheva, N.T.; Morris, J.H.; Bork, P.; et al. STRING v11: Protein-protein association networks with increased coverage, supporting functional discovery in genome-wide experimental datasets. *Nucleic Acids Res.* **2019**, *47*, 607–613. [[CrossRef](#)]
28. Warde-Farley, D.; Donaldson, S.L.; Comes, O.; Zuberi, K.; Badrawi, R.; Chao, P.; Franz, M.; Grouios, C.; Kazi, F.; Lopes, C.T.; et al. The GeneMANIA prediction server: Biological network integration for gene prioritization and predicting gene function. *Nucleic Acids Res.* **2010**, *38*, W214–W220. [[CrossRef](#)]
29. Vasaikar, S.V.; Straub, P.; Wang, J.; Zhang, B. LinkedOmics: Analyzing multi-omics data within and across 32 cancer types. *Nucleic Acids Res.* **2018**, *46*, D956–D963. [[CrossRef](#)]
30. Ru, B.; Wong, C.N.; Tong, Y.; Zhong, J.Y.; Zhong, S.S.W.; Wu, W.C.; Chu, K.C.; Wong, C.Y.; Lau, C.Y.; Chen, I.; et al. TISIDB: An integrated repository portal for tumor-immune system interactions. *Bioinformatics* **2019**, *35*, 4200–4202. [[CrossRef](#)]
31. Vousden, K.H.; Prives, C. p53 and prognosis: New insights and further complexity. *Cell* **2005**, *120*, 7–10. [[PubMed](#)]
32. Chu, B.; Kon, N.; Chen, D.; Li, T.; Liu, T.; Jiang, L.; Song, S.; Tavana, O.; Gu, W. ALOX12 is required for p53-mediated tumour suppression through a distinct ferroptosis pathway. *Nat. Cell Biol.* **2019**, *21*, 579–591. [[CrossRef](#)] [[PubMed](#)]
33. Morris, J.P., IV; Yashinski, J.J.; Koche, R.; Chandwani, R.; Tian, S.; Chen, C.C.; Baslan, T.; Marinkovic, Z.S.; Sánchez-Rivera, F.J.; Leach, S.D.; et al.  $\alpha$ -Ketoglutarate links p53 to cell fate during tumour suppression. *Nature* **2019**, *573*, 595–599. [[CrossRef](#)] [[PubMed](#)]
34. Spike, B.T.; Wahl, G.M. p53, Stem Cells, and Reprogramming: Tumor Suppression beyond Guarding the Genome. *Genes Cancer* **2011**, *2*, 404–419. [[CrossRef](#)]
35. Janic, A.; Valente, L.J.; Wakefield, M.J.; Di Stefano, L.; Milla, L.; Wilcox, S.; Yang, H.; Tai, L.; Vandenberg, C.J.; Kueh, A.J.; et al. DNA repair processes are critical mediators of p53-dependent tumor suppression. *Nat. Med.* **2018**, *24*, 947–953. [[CrossRef](#)]
36. Blagih, J.; Zani, F.; Chakravarty, P.; Hennequart, M.; Pilley, S.; Hobor, S.; Hock, A.K.; Walton, J.B.; Morton, J.P.; Gronroos, E.; et al. Cancer-Specific Loss of p53 Leads to a Modulation of Myeloid and T Cell Responses. *Cell Rep.* **2020**, *30*, 481–496. [[CrossRef](#)]
37. Biegging-Rolett, K.T.; Kaiser, A.M.; Morgens, D.W.; Boutelle, A.M.; Seoane, J.A.; Van Nostrand, E.L.; Zhu, C.; Houlihan, S.L.; Mello, S.S.; Yee, B.A.; et al. Zmat3 Is a Key Splicing Regulator in the p53 Tumor Suppression Program. *Mol. Cell* **2020**, *80*, 452–469. [[CrossRef](#)]
38. Zhou, G.; Liu, Z.; Myers, J.N. TP53 Mutations in Head and Neck Squamous Cell Carcinoma and Their Impact on Disease Progression and Treatment Response. *J. Cell. Biochem.* **2016**, *117*, 2682–2692. [[CrossRef](#)]
39. Cancer Genome Atlas Network. Comprehensive genomic characterization of head and neck squamous cell carcinomas. *Nature* **2015**, *517*, 576–582. [[CrossRef](#)]
40. Caponio, V.C.A.; Troiano, G.; Adipietro, I.; Zhurakivska, K.; Arena, C.; Mangieri, D.; Mascitti, M.; Cirillo, N.; Lo Muzio, L. Computational analysis of TP53 mutational landscape unveils key prognostic signatures and distinct pathobiological pathways in head and neck squamous cell cancer. *Br. J. Cancer* **2020**, *123*, 1302–1314. [[CrossRef](#)]
41. Perrone, F.; Bossi, P.; Cortelazzi, B.; Locati, L.; Quattrone, P.; Pierotti, M.A.; Pilotti, S.; Licitra, L. TP53 mutations and pathologic complete response to neoadjuvant cisplatin and fluorouracil chemotherapy in resected oral cavity squamous cell carcinoma. *J. Clin. Oncol.* **2010**, *28*, 761–766. [[CrossRef](#)]
42. Jagla, W.; Wiede, A.; Hinz, M.; Dietzmann, K.; Gülicher, D.; Gerlach, K.L.; Hoffmann, W. Secretion of TFF-peptides by human salivary glands. *Cell Tissue Res.* **1999**, *298*, 161–166. [[CrossRef](#)] [[PubMed](#)]
43. Kouznetsova, I.; Kalinski, T.; Peitz, U.; Mönkemüller, K.E.; Kalbacher, H.; Vieth, M.; Meyer, F.; Roessner, A.; Malfertheiner, P.; Lippert, H.; et al. Localization of TFF3 peptide in human esophageal submucosal glands and gastric cardia: Differentiation of two types of gastric pit cells along the rostro-caudal axis. *Cell Tissue Res.* **2007**, *328*, 365–374. [[CrossRef](#)] [[PubMed](#)]
44. Hoffmann, W. Trefoil Factor Family (TFF) Peptides and their Different Roles in the Mucosal Innate Immune Defense and More: An Update. *Curr. Med. Chem.* **2021**, *28*, 7387–7399. [[CrossRef](#)]
45. Jahan, R.; Shah, A.; Kisling, S.G.; Macha, M.A.; Thayer, S.; Batra, S.K.; Kaur, S. Odyssey of trefoil factors in cancer: Diagnostic and therapeutic implications. *Biochim. Biophys. Acta (BBA)—Rev. Cancer* **2020**, *1873*, 188362. [[CrossRef](#)] [[PubMed](#)]
46. Cui, H.Y.; Wang, S.J.; Song, F.; Cheng, X.; Nan, G.; Zhao, Y.; Qian, M.R.; Chen, X.; Li, J.Y.; Liu, F.L.; et al. CD147 receptor is essential for TFF3-mediated signaling regulating colorectal cancer progression. *Signal Transduct. Target. Ther.* **2021**, *6*, 268. [[CrossRef](#)] [[PubMed](#)]

47. Liu, J.; Kim, S.Y.; Shin, S.; Jung, S.H.; Yim, S.H.; Lee, J.Y.; Lee, S.H.; Chung, Y.J. Overexpression of TFF3 is involved in prostate carcinogenesis via blocking mitochondria-mediated apoptosis. *Exp. Mol. Med.* **2018**, *50*, 1–11. [[CrossRef](#)]
48. Yang, L.; Zhang, X.; Zhang, J.; Liu, Y.; Ji, T.; Mou, J.; Fang, X.; Wang, S.; Chen, J. Low expression of *TFF3* in papillary thyroid carcinoma may correlate with poor prognosis but high immune cell infiltration. *Future Oncol.* **2022**, *18*, 333–348. [[CrossRef](#)] [[PubMed](#)]
49. Nisar, S.; Yousuf, P.; Masoodi, T.; Wani, N.A.; Hashem, S.; Singh, M.; Sageena, G.; Mishra, D.; Kumar, R.; Haris, M.; et al. Chemokine-Cytokine Networks in the Head and Neck Tumor Microenvironment. *Int. J. Mol. Sci.* **2021**, *22*, 4584. [[CrossRef](#)]
50. Fridman, W.H.; Zitvogel, L.; Sautès-Fridman, C.; Kroemer, G. The immune contexture in cancer prognosis and treatment. *Nat. Rev. Clin. Oncol.* **2017**, *14*, 717–734. [[CrossRef](#)]
51. Gentles, A.J.; Newman, A.M.; Liu, C.L.; Bratman, S.V.; Feng, W.; Kim, D.; Nair, V.S.; Xu, Y.; Khuong, A.; Hoang, C.D.; et al. The prognostic landscape of genes and infiltrating immune cells across human cancers. *Nat. Med.* **2015**, *21*, 938–945. [[CrossRef](#)] [[PubMed](#)]